International Journal of Peptide Research and Therapeutics (2023) 29:84
https://doi.org/10.1007/s10989-023-10556-9

Heterologous Expression and Initial In Silico Characterization of a Novel Snakin-Z Peptide

Tuğba Teker[1] · Gülruh Albayrak[2] · Kadir Turan[3]

Accepted: 21 July 2023

Abstract

Heterologous expression of the plant-derived snakin-Z (SNK-Z) peptide was carried out in *Escherichia coli* BL21 and Mach 1 strains using the pET14b, and pGEX-6P-1 vectors, and its tertiary structure was determined. The most efficient production of the recombinant fusion peptide (GST/SNK-Z) in both strains was achieved by induction with 0.1 mM isopropyl β-D-1-thiogalactopyranoside at 32 °C. GST/SNK-Z with 30.14 kDa which yielded 6.5 mg/L protein, was purified by affinity chromatography followed by dialysis. The GST tags were removed using PreScission protease. The IC_{50} of GST/SNK-Z was calculated as 12.07 µM for *Staphylococcus aureus* (ATCC 25923) using nonlinear regression analysis. The secondary structure of recombinant SNK-Z consisted of α-helix and coil sites. It's 3-D model was generated with a confidence score of -0.20 and a template modeling score of 0.69 ± 0.12. The predicted solvent accessibility and B-factor profile were detected.

This is the first report of heterologous expression of SNK-Z in *E. coli*. Our study provides fundamental data for the large-scale production of SNK-Z, which has a high potential for use in the pharmaceutical industry because of its previously reported antimicrobial effects.

Keywords Antimicrobial peptide · *Escherichia coli* · Heterologous expression · Snakin-Z

Introduction

The broad-range resistance mechanisms acquired by pathogenic microorganisms against antibiotics have led to the discovery of novel compounds with antimicrobial effects. Antimicrobial peptides (AMPs), usually consisting of 10–100 amino acids, are produced by all living organisms (bacteria, archaea, protozoa, fungi, plants, and animals) as part of the host defense (Zhang et al. 2021). They are considered natural antibiotic candidates because they have a high potential to replace antibiotics in the fight against pathogenic microorganisms, especially multidrug-resistant ones (Wang 2020; Su et al. 2020). To date, more than 2000 AMPs have been identified in various organisms, from bacteria to animals, including humans. AMPs display various biological activities (e.g., antibacterial, antifungal, antiviral, antiparasitic, insecticidal, immunomodulatory, antibiofilm, and anticancer). Therefore, they have the potential to be used in the agricultural, medical, cosmetic, and food industries. Because the majority of these peptides function as signaling molecules in plants, they are effective in adapting to rapidly changing environmental conditions, in resistance to herbivores and/or pathogen attacks, and in the evolution of plants (Wheeler and Irving 2012). Information on these peptides and their characteristics can be obtained from several

✉ Gülruh Albayrak
gulruh@istanbul.edu.tr

Tuğba Teker
tugba.teker@ogr.iu.edu.tr

Kadir Turan
kadirturan@marmara.edu.tr

[1] Programme of Molecular Biotechnology and Genetics, Institute of Graduate Studies in Sciences, Istanbul University, Süleymaniye, Istanbul 34116, Turkey

[2] Department of Molecular Biology and Genetics, Faculty of Sciences, Istanbul University, Vezneciler, Istanbul 34134, Turkey

[3] Department of Basic Pharmaceutical Sciences, Faculty of Pharmacy, Marmara University, Başıbüyük, Istanbul 34854, Turkey

Published online: 01 August 2023

web-based repositories [1,2,3]. AMPs are grouped according to their source organisms, biological activities, peptide features (net charge, length, hydrophobicity ratio, amino acid sequence similarities, chemical modifications, unique sequence motifs, and three-dimensional (3-D) structures), and mechanisms of action. 3-D structures, presence of cysteine (cys) motifs, and amino acid sequence homologies are important criteria in the classification of plant AMPs (Li et al. 2021). They are mainly classified as defensins, thionins, lipid transfer proteins (LTPs), cyclotides, hevein-like peptides, knottins, α-hairpinins, and snakins (Su et al. 2020).

Snakin-Z (SNK-Z) is an AMP identified from *Zizyphus jujuba* fruits and included in the defensin-like snakin-2 group. It inhibits the growth of various bacterial and fungal pathogens such as *Bacillus subtilis*, *Klebsiella pneumoniae*, *Staphylococcus aureus*, *Aspergillus niger*, *Candida albicans*, *Phomopsis azadirachtae*, and *Pythium ultimum*. The antimicrobial properties of SNK-Z make it an appropriate candidate for the design of novel therapeutics (Daneshmand et al. 2013).

Once AMPs are isolated from their natural sources, they must be purified and characterized. Extraction from natural sources is a complicated and costly process. Routinely used extraction and purification methods do not allow sufficient AMP to be obtained from crude biological samples. Large amounts of crude biological samples must be used to obtain limited quantities of peptides. Chemical synthesis of these peptides at high purity and yield is an alternative and rapid approach; however, the chemical synthesis of a custom-designed AMP in small quantities is expensive. Therefore, the utilization of AMPs in commercial applications and scale-up processes is limited. The production of AMPs via heterologous gene expression has great advantages over other approaches, as it is a sustainable, scalable, and economically feasible strategy. AMPs are generally expressed as fusion proteins that facilitate their purification in heterologous expression systems. *E. coli* and *B. subtilis* from prokaryotic organisms and *Pichia pastoris*, *Saccharomyces cerevisiae* from eukaryotic ones have commonly used host microorganisms in the heterologous production of AMPs.

It was aimed to produce SNK-Z peptide in *E. coli* BL21 and Mach 1 strains using heterologous gene expression systems for the first time, in this study. To understand the structural properties of recombinant SNK-Z, structural models were estimated using *in silico* methods, and the data will contribute to further molecular docking analysis. Whether the recombinant peptide is a suitable candidate for utilization in the pharmaceutical and cosmetic industries is also discussed.

Materials and Methods

Bacterial Transformation and Selection

Subcloning of the coding sequences of the SNK-Z peptide was performed in the *E. coli* Mach 1 strain. *E. coli* BL21 (DE3; Novagen) and Mach 1 strains were used as the host cells for SNK-Z expression. pET-14b (Novagen) and pGEX-6P-1 (GE Healthcare) were used to construct expression vectors. Bacterial cultures were grown overnight in LB (Luria-Bertani) broth and LB broth containing 50 µg ampicillin mL^{-1} at 37 °C on an orbital shaker (180 rpm; shaking). All bacterial stocks were stored at -80 °C in LB medium supplemented with 25% glycerol.

Retrieval and Construction of Nucleotide Sequences Encoding SNK-Z Peptide

The amino acid sequence of the SNK-Z peptide was retrieved from the APD[4]. The oligonucleotide sequence responsible for the synthesis of the selected AMP was obtained by "reverse translation" of the SNK-Z amino acid sequences. The 93-base sequence was rearranged according to codon preference of *E. coli* using the "Sequence Manipulation Suite" program. Additional nucleotides (5'-TAT-3') were added to the 5' end of the coding strand to maintain the reading frame of *E. coli* and construct the SNK-Z-integrated pET-14b vector. Both forward and reverse primer sequences for SNK-Z were commercially synthesized by Ella Biotech (Table 1). Synthetic SNK-Z fragments (30 pM/µL) were phosphorylated with T4 polynucleotide kinase (NEB, #0201) (0.5 U/µL) in a total volume of 20 µL at 37 °C for 1 h. Phosphorylated double-stranded SNK-Z fragments were obtained by keeping the samples at 95 °C for 2 min and cooling them to 30 °C (20% ramp value) in a thermal cycler.

Construction of Recombinant Plasmid Vectors

Recombinant pET-14b-SNK and pGEX-6P-1-SNK vectors were constructed by inserting double-stranded SNK-Z fragments into pET-14b and pGEX-6P-1, respectively (Fig. 1). The pET-14b vector was digested with *Nde*I (Thermo Fisher Scientific, #ER0581). Klenow fragment (NEB, #M0210) was used to generate a blunt-ended plasmid by filling 5′-overhangs of linear pET-14b. Dephosphorylation of the

[1] https://aps.unmc.edu/.

[2] http://www.yadamp.unisa.it.

[3] www.camp3.bicnirrh.res.in.

[4] https://aps.unmc.edu/.

Table 1 Primers used in this study

Primer	Sequence (5'-3')
megaF	TATGCGCGCGCCTGAACTGCGTGC-CGAAAGGCACCAGCGGCAACACC-GAAACCTGCCCGTGCTATGCGAGCCT-GCATAGCTGCCGCAAATATGGCTAA
megaR	TTAGCCATATTTGCGGCAGCTATGCAG-GCTCGCATAGCACGGGCAGGTTTCG-GTGTTGCCGCTGGTGCCTTTCGGCAC-GCAGTTCAGGCGCGCGCATA
SnaF	CTGCGCGCGCCTGAACTGCG
SnaR	TTAGCCATATTTGCGGCAGCTATG
pET-sqF*	AGGGAGACCACAACGGTTTC
pET-sqR*	TGGCAGCAGCCAACTCAGC
pGEXF**	GGGCTGGCAAGCCACGTTTGGTG
pGEXR**	CCGGGAGCTGCATGTGTCAGAGG

F: forward, R: reverse primers, * Specific to pET-14b, ** Specific to pGEX-6P-1

blunt ends was carried out with shrimp alkaline phosphatase (SAP) (Thermo Fisher Scientific, #EF0651) by incubation at 37 °C for 1 h, and the reaction was stopped at 65 °C for 20 min. The recombinant pET-14b-SNK vector was constructed by ligating the SNK-Z fragment to pET-14b with T4 DNA ligase (Invitrogen, #15-224-041) at 20 °C for 16 h. The SNK-Z coding sequence was amplified from the constructed pET-14b-SNK vector to integrate it into the pGEX-6P-1 vector system using primers designed to avoid changing the open reading frame of AMP. The primer pairs (snaF/R) (Table 1), were phosphorylated as previously described. PCR amplification was carried out using high-fidelity 2xHF PCR MasterMix (Episozyme, #EZ-HF01) under the following conditions: pre-denaturation step (1 cycle) at 95 °C for 2 min; 30 cycles of denaturation at 95 °C for 10 s, annealing at 58 °C for 10 s, extension at 74 °C for 15 s, and a final extension step at 74 °C for 5 min. The pGEX-6P-1 plasmid (5 µg) was digested overnight with *Bam*HI (NEB, #R0136) in a total volume of 100 µL at 37 °C, blunted with the Klenow fragment, and then dephosphorylated with SAP. Ligation was performed using T4 DNA ligase, as described above.

Plasmid Vectors, Bacterial Strains and Culture Conditions

The transformation of plasmids into chemically competent *E. coli* Mach 1 and BL21 (DE3) cells were carried by heat-shock method (Chang et al. 2017). Transformants were selected via colony PCR using different combinations of vector-specific universal primers (pET-sqF/R and pGEXF/R) and oligonucleotide primers targeting the coding sequence (Table 1). Positive colonies carrying the pET-14b-SNK and pGEX-6P-1-SNK vectors were cultured in LB broth (+amp) at 37 °C by shaking overnight at 180 rpm. Once their plasmid DNAs were isolated, the recombinant plasmids were verified by Sanger sequencing. Transformants carrying the pET-14b and pGEX-6P-1 vectors were used as negative controls to confirm recombinant peptide production.

Expression of the Fusion Peptide in *E. coli*

Transformant colonies carrying the pET-14b-SNK and pGEX-6P-1-SNK plasmids were individually inoculated overnight in 5-500 mL LB broth (+amp) at 37 °C with shaking (180 rpm). The optimal incubation temperature for bacterial hosts and optimal inducer concentration for gene expression were determined to obtain the most efficient protein production in cultures. The cultures were grown at 32 or 37 °C. When the cell density reached OD_{600} ~ 0.6,

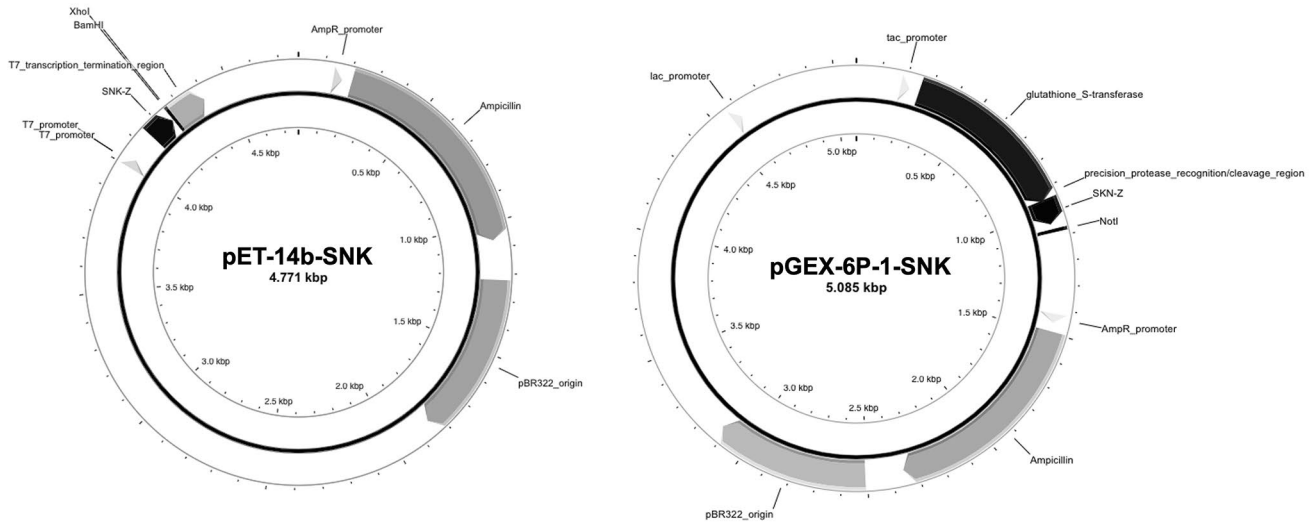

Fig. 1 Schematic representation of pET-14b-SNK and pGEX-6P-1-SNK plasmids (Created using PlasMapper 3.0)

isopropyl-β-D-thiogalactoside (IPTG) was added to the cultures at different concentrations (0.05 mM, 0.1 mM, and 0.2 mM) to induce recombinant protein expression. The cultures were then incubated for an additional 5 h. The expression of the fusion peptide in the cells was analyzed using 10–15% acrylamide SDS-PAGE. The cells in the culture were precipitated by centrifugation at 8000 rpm for 5 min and lysed in SDS loading buffer. After denaturation at 95 °C for 5 min, total lysates were subjected to SDS-PAGE Electrophoresis was performed at 40 V for 15 min and then at 80 V for 60–75 min for each gel (10 × 10 × 1 mm). The proteins separated on the gel were visualized using silver staining based on the method described by Merril et al. (1981).

Isolation and Purification of Recombinant Proteins

The cells in saturated cultures of 500 mL LB medium were precipitated by centrifugation at 8000 g for 12 min. The cell pellets were resuspended in 2–4 mL lysis buffer (5 mM DTT, 0.1% NP40, 0.1 mM PMSF, 50 mM Tris, 150 mM sodium chloride, pH 7.0). The cell suspension was lysed by sonication (15 s pulses with intervals of 15 s each, at 85% amplitude) for 10 min on ice. The lysates were centrifuged at 13000 g for 15 min to remove cell debris. The concentration of proteins in the supernatant was determined using the Bradford assay (Bio-Rad) (Bradford 1976). The soluble protein extract was then used for fusion protein purification. The GST-tagged fusion protein was purified by affinity chromatography using Pierce™ Glutathione Agarose (Thermo), according to the manufacturer's instructions, and eluted proteins were analyzed by SDS-PAGE.

The purified fusion protein with the N-terminal GST tag was digested with PreScission protease to remove the GST tag from the Leu-Glu-Val-Leu-Phe-Gln/Gly-Pro region. GST fusion proteins were cleaved in a buffer containing 50 mM Tris-HCl (pH 7.0), 150 mM NaCl, 1mM EDTA and 1mM DTT at 4 °C for 16 h. 1U enzyme was used for each 100 µg of fusion sample.

Dialysis and Lyophilization of Purified GST/SNK-Z

Dialysis of GST/SNK-Z was performed using "Regenerated Cellular Dialysis Tubing" (Orange Scientific). The membrane, which was stored at 4 °C in a 50% ethanol/1 mM EDTA mixture, was transferred into distilled water and kept in a magnetic stirrer for 5 min. Then the protein sample was transferred into the membrane. The membrane was kept in 1000 mL of distilled water for 20 h (Supplementary Fig. 1A) [Supplementary Information (SI)]. During the process, water was re-filled 2 times. The GST/SNK-Z were transferred to 2 mL polypropylene tubes and they were lyophilized (Supplementary Fig. 1B) [SI]. Dry weights of the lyophilized samples were measured with precision scales. GST/SNK-Z samples were dissolved in phosphate buffered saline (PBS) and run in SDS-PAGE. Silver staining was performed as previously described above.

Western Blot Analysis

Western blotting was performed using anti-GST antibodies to verify the expression of the fusion peptide. Samples were separated by 10% SDS-PAGE, and the proteins were transferred onto a nitrocellulose membrane under wet conditions in cold transfer buffer (25 mM Tris-HCl, 192 mM glycine, pH 8.3, 20% methanol (v/v), and 0.01% SDS) at 45 V for 45 min and 90 V for 90 min. Subsequently, the membrane was blocked with 5% milk powder in TBS-T (5% milk powder, 10 mM Tris, 100 mM NaCl, and 0.05% Tween-20; pH 7.4). After blocking, the membrane was first treated with mouse monoclonal anti-GST (1:2000) (Abcam, ab9085) overnight and then labeled with a secondary antibody conjugated with horseradish peroxidase, anti-mouse IgG-HRP (Invitrogen/ Thermo, #31423) (titer 1:500) for 45 min. The proteins were visualized with a gel imaging system (DNR Bio-Imaging system) using a chemiluminescence substrate (H&C, RPN2232).

Antibacterial Activity of Purified GST/SNK-Z

S. aureus (ATCC 25923) was used to test the antibacterial properties of GST/SNK-Z using microdilution assays at five different concentrations (12.5, 25, 50, 100, 150 µM). *S. aureus* was grown in 10 mL Müller Hington Broth (MHB) overnight at 37 °C. The turbidity of the cultures was adjusted to McFarland standard 0.5 (optical density at 625 nm should be at 0.08–0.13) with MHB. The final inoculum size was adjusted to 5×10^5 colony formation units (cfu)/mL in order to standardize the inoculum for antibacterial activity according to CLSI guidelines. After the GST/SNK-Z was sterilized by filtration through a 0.2 µm membrane filter, the fusion molecule was pipetted into the well. The final concentration of GST/SNK-Z ranged from 0 to 150 µM. The experiment was performed in a total volume of 200 µL cation-adjusted MHB. The well plates were incubated at 35 °C for 16 h by sealed with laboratory parafilm to avoid evaporation of the samples. Antibacterial activity was determined by measuring the absorbance of the samples at 600 nm. Non-treated cation-adjusted MHB was used as a blank and GST/SNK-Z treated MHB was used as a sterility control. Bacterial growth was determined using the formula "Cell viability = [(At)/Ac] × 100", where Ac was measured absorbance of the untreated controls at 600 nm, and At was measured absorbance of the samples. The GST/SNK-Z concentration required to inhibit 50% of growth (IC_{50}) was estimated by

statistical analysis using GraphPad Prism 9.0 (Wirjanata et al. 2016). The experiment was performed in quadruplicates.

In Silico Analysis of Recombinant SNK-Z

The theoretical isoelectric point (pI) and molecular weight (MW) of the peptides were determined using the ExPASy Compute pl/Mw tool[5]. The ExPASy translate tool[6] was used to predict the translation of nucleotide sequences to amino acid sequences of the protein. The secondary and tertiary structures of recombinant SNK-Z peptide together with solvent accessibility and normalized B-factor were estimated via I-TASSER (Iterative Threading ASSEmbly Refinement)[7]. The model predicted by I-TASSER was visualised using PyMOL software.

Results and Discussion

Construction of Recombinant Vectors

Heterologous expression of SNK-Z, a herbal-originated AMP, was successfully carried out in *E. coli*. Although heterologous expression of polypeptides using bacterial hosts is faster, easier, and more broadly applicable than other eukaryotic expression systems, such as *Pichia pastoris*, it can result in the production of insoluble and non-functional proteins. Moreover, AMPs produced in this manner have a high potential to be toxic to bacterial hosts. It is therefore preferable to synthesize the peptide of interest as fusion partners to increase solubility and avoid toxicity to host cells (Harper and Speicher 2011; Herbel et al. 2015). Fusion systems can also be used to purify recombinant proteins from bacterial cell lysates (Jeyarajan et al. 2023). In this study, pET-14b, which carries an N-terminal His•Tag sequence followed by a thrombin cleavage site, and pGEX-6P-1 vectors that express GST fusion proteins with a PreScission protease site were used as fusion partners for enhanced protein purification.

The pET-14b-SNK (4.771 kbp) vector was constructed by inserting peptide-coding sequences to upstream of the thrombin region using the *Nde*I restriction enzyme. The position of the SNK-Z fragment in the vector was verified through DNA sequencing (Supplementary Fig. 2) [SI]. In the pGEX-6P-1 vector system, the 97 bp SNK-Z coding sequence amplified from the pET-14b-SNK vector by PCR was cloned to the downstream of the GST coding sequence. The recombinant vectors were transferred into *E. coli* BL21 (DE3) and *E. coli* Mach 1 cells. Colonies containing the pGEX-6P-1-SNK with 5.085 kbp were confirmed by restriction digestion, and the position of the insert DNA within the vectors was confirmed by DNA sequencing (Supplementary Fig. 3) [SI].

Heterologous Expression of SNK-Z

The pET-14b-SNK and pGEX-6P-1-SNK recombinant vectors were used to express the SNK-Z fragment as a fusion protein. pET-14b-SNK and pGEX-6P-1-SNK were individually introduced into chemically competent *E. coli* BL21 (DE3) cells; however, only Mach1 was used as an expression host for the pGEX-6P-1-SNK vector. Transcription of target genes in the pET expression vector series is controlled by under the T7 promoter region. The *E. coli* BL21 (DE3) strain, which contains a chromosomal copy of the T7 RNA polymerase gene under lacUV5 control, is therefore a suitable expression host for the production of heterologous peptides from SNK nucleotide sequences inserted into the pET vector. pGEX expression vectors are GST tagging vectors, and their expression is under the control of the tac promoter, which is modified from the promoters of tryptophan and lactose operons induced by IPTG. Protein expression is induced by the addition of IPTG, a non-metabolizable lactose analog, to the bacterial culture in both vector systems. With the ExPASy Compute pl/Mw tool, the theoretical pI of fusion peptides to be produced in host cells carrying the pET-14b-SNK and pGEX-6P-1-SNK vectors were estimated to be 9.04 and 6.39, respectively, so the net charge of His/SNK-Z was positive at pH 7.0, and negative for GST/SNK-Z. The molecular mass of the fusion peptide to be produced in host cells carrying pET-14b-SNK was estimated 5.6 kDa and that of the host carrying pGEX-6P-1-SNK was 30.14 kDa. Expression of GST fused peptide (GST/SNK-Z) with 30.14 kDa size and 26 kDa GST molecules were visualized in both BL21 (DE3) and Mach 1 cells cultured in 500 mL LB (+amp) medium (Fig. 2). The pGEX gene fusion vectors allowed us to visualize the production of low-molecular-weight proteins because they are included a region for the synthesis of 26-kDa GST encoded by the parasitic helminth *Schistosoma japonicum*.

When the effects of IPTG concentration and incubation temperature on protein expression were evaluated, the optimal parameters were determined to be expression at 32 °C for 4-h after induction with 0.1 mM IPTG in both strains (Figs. 3 and 4 A-B). Synthesis of the fusion peptide in bacterial cells was also examined by Western blot analysis (Fig. 5). The GST-fused SNK-Z peptide was obtained with high purity by using GST pull-down assay. Purity of the GST-fused SNK-Z peptide after GST pull-down assay and dialysis was shown in Fig. 6A and B, respectively. The

[5] https://web.expasy.org/compute_pi/.

[6] https://web.expasy.org/translate/.

[7] https://zhanggroup.org/I-TASSER/.

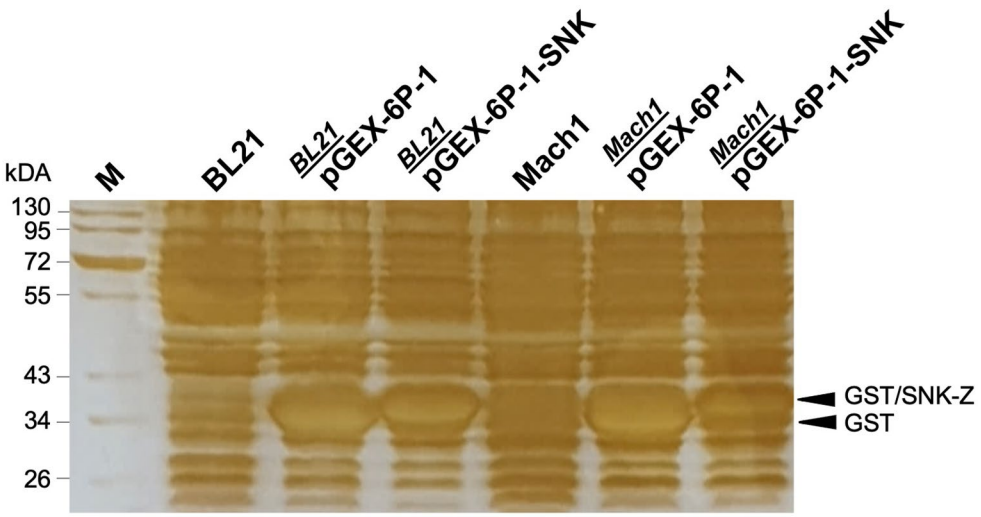

Fig. 2 SDS-PAGE analysis of GST and GST/SNK-Z expression encoded by pGEX-6P-1 and pGEX-6P-1-SNK plasmids in *E. coli* cells. M: Prestained protein marker, broad range marker (NEB, P7719S)

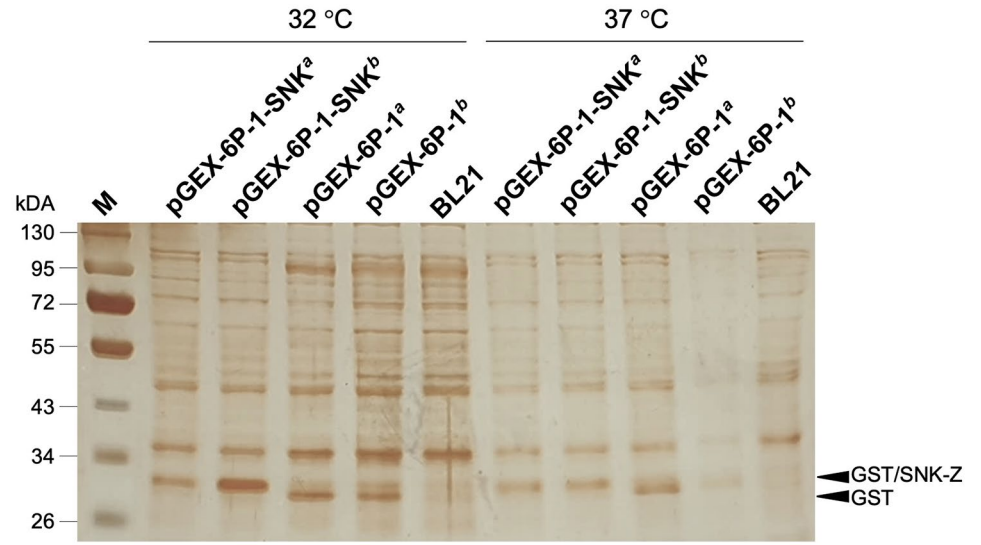

Fig. 3 GST and GST/SNK-Z expression in *E. coli* BL21 cells cultured at different temperatures (32 and 37 °C) induced with different concentrations of IPTG ([a] 0.2 and [b] 0.1 mM). M: Prestained protein marker, broad range marker (NEB, P7719S)

average yield of purified fusion protein after dialysis was calculated to be 6.5 mg/L. The results showed that the GST tag is a highly efficient fusion tag for purifying GST/SNK-Z from bacterial cell lysates. Herbel et al. (2015) could not be able to separate the low mass recombinant snakin-2 peptide from the fusion molecule with thioredoxin. They evaluated antibacterial activity of the mixture of these two proteins. In various studies, in which GST was used as a fusion partner for recombinant protein expression, the antimicrobial effect of the fusion molecule was investigated (Yu et al. 2016; Cao et al. 2021; Taghizadeh et al. 2022). GST tags have been reported to have no effect on the function and structure of antimicrobial peptides (Yu et al. 2016; Taghizadeh et al. 2022). Since individual recombinant SNK-Z could not be visualized by SDS-PAGE after proteolytic cleavage (Fig. 6C), and SNK-Z could potentially show inhibitory effects against pathogens without the need for GST-tag cleavage, the antimicrobial activity of GST/SNK-Z was evaluated, similar to the studies in which antibacterial activity of GST-fused antibacterial peptide was assayed. *S. aureus* growth after treatment was decreased in dose dependent manner. IC_{50} reflects the measure of its effectiveness in inhibiting biological or biochemical functions; therefore, it is an important measure of potency for a given substance. The IC_{50} of GST/SNK-Z was calculated as 12.07 µM for the *S. aureus* reference strain by nonlinear regression of growth inhibition caused by different concentrations of GST/SNK-Z (Fig. 7). The estimated IC_{50} values against *S. aureus* in the present study are higher than MIC of previously reported SNK-Z as 28 µg/mL which corresponds to 8.68 µM (Daneshmand et al. 2013).

The expected fragment belonging to the 5.6 kDa fusion peptide that was produced from BL21 transformants carrying pET-14b-SNK that was grown by stimulation with

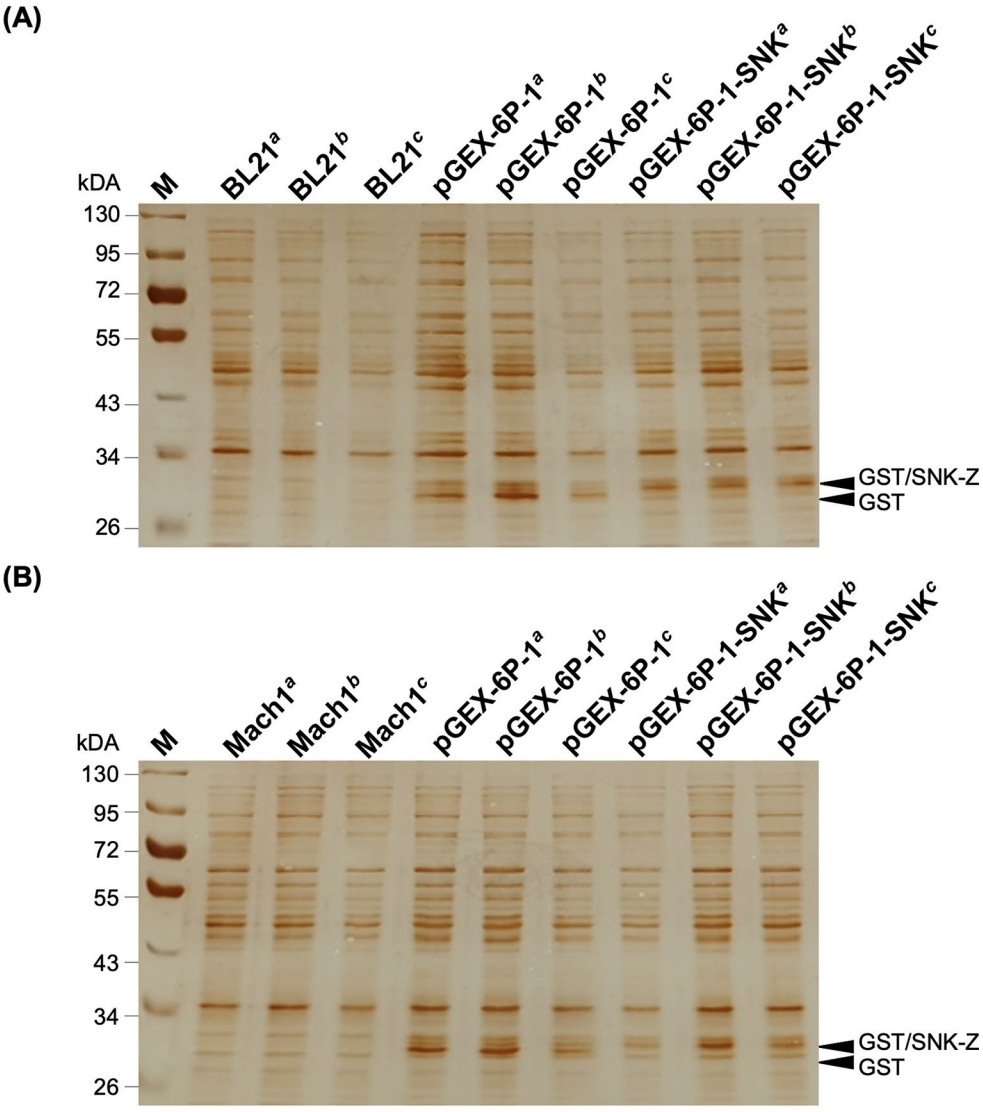

Fig. 4 GST and GST/SNK-Z expression in BL21 **(A)** and Mach 1 **(B)** strains cultured at 32 °C and induced with different IPTG concentrations. [a] 50 µM,[b] 100 µM, [c] 200 µM final concentration of IPTG. M: Prestained protein marker, broad range marker (NEB, P7719S)

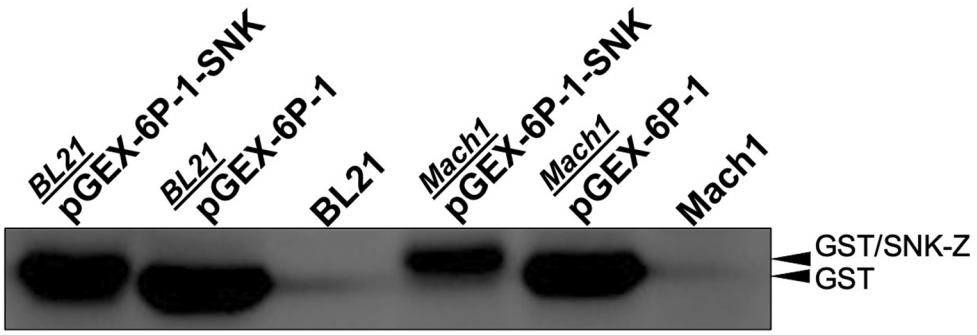

Fig. 5 Western blot analysis of GST/SNK-Z proteins expressed in BL21 and Mach1 strains. The proteins were labeled with rabbit polyclonal anti-GST and HRP conjugated goat anti-rabbit IgG, and visualized with an ECL Western blotting detection kit (GE Healthcare)

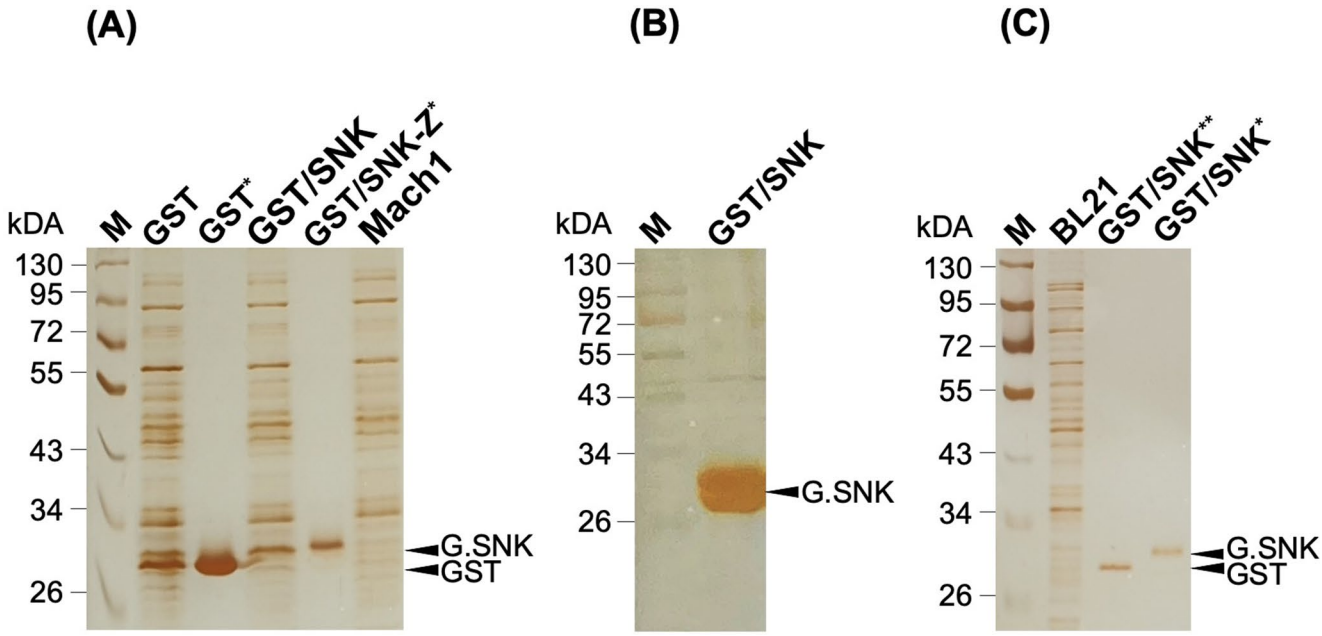

Fig. 6 The analysis of affinity purified and protease cleaved GST/SNK-Z with SDS PAGE **(A)** The proteins expressed in Mach 1 transformed with plasmid DNAs indicated in figure, line 1: total proteins of pGEX-6P-1/Mach 1; line 2: purified GST (from pGEX-6P-1/Mach 1); line 3: total proteins of pGEX-6P-1-SNK/Mach 1; line 4: purified GST/SNK-Z (from pGEX-6P-1-SNK/Mach 1); line 5: total proteins of Mach 1. **(B)** GST/SNK-Z after dialysis. **(C)** The protein expressed in BL21 transformed with plasmid DNAs indicated in figure, line 1: total proteins of BL21; line 2: purified and protease cleaved GST/SNK-Z (from pGEX-6P-1-SNK/BL21); line 3: purified, non-cleaved GST/SNK-Z from pGEX-6P-1-SNK/BL21). M: Prestained protein marker, broad-range marker (NEB, P7719S). *Precipitated by glutathione agarose, **cleaved with PreScission protease

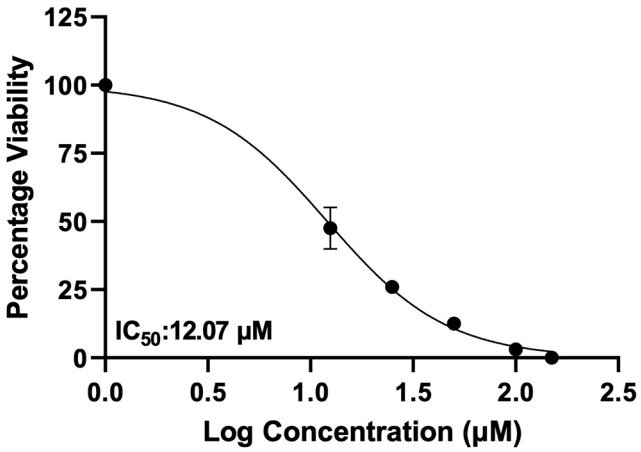

Fig. 7 IC_{50} determined by nonlinear regression from logarithmic concentrations of GST/SNK-Z versus normalized response with variable slope. Bars represent means ± SEM.

different concentrations of IPTG at two different incubation temperatures could not be observed in polyacrylamide gel (data not shown). According to the results, the GST-tagged fusion vector system is more suitable than the his-tagged expression vector for the expression of low-molecular-weight peptides. Our results were consistent with the literature that reported GST could be a preferable fusion partner for soluble expression in *E. coli* because it facilitates the production of soluble and active recombinant proteins (Taghizadeh et al. 2022).

In Silico Analysis of Recombinant SNK-Z Structure

AMPs of the snakin family have been identified in a wide range of plant species. Annotated 3-D protein models of different snakins, generated by automated homology modeling, can be accessed via SWISS-MODEL[8]. Snakin-1 (UniProt: Q948Z4) and snakin-2 (Uniprot: Q93X17) peptides isolated from potato tubers have been the most extensively studied members of the snakin/GASA family (Segura et al. 1999; Berrocal-Lobo et al. 2002). Snakins are composed of three distinct regions: N-terminal signal peptide, variable, and C-terminal regions. The C-terminal region carries a GASA domain consisting of 12 cys residues in conserved positions that contribute to the biochemical stability of the molecule. The variable region displays high diversity among members of the snakin family with respect to the composition and sequence length of amino acids (Yeung et al. 2016; Su et al. 2020). Although the 12 characteristic cys, residues are highly conserved throughout the family, defined amino acid sequences of SNK-Z lack a certain number of cys residues.

[8] https://swissmodel.expasy.org/repository?start=0&rows=50&query=snakin.

The 3-D structure of proteins allows for the design of novel and more effective antimicrobial agents (Liu et al. 2018). I-TASSER server is an integrated platform to predict structures and functions of proteins based on "the sequence-to-structure-to-function paradigm". The program is initiated using an amino acid sequence. The secondary structure, which can be used to estimate the number of secondary structure elements and tertiary structure class of the query protein, was predicted using I-TASSER. The predicted secondary structure of recombinant SNK-Z contained a mixture of α-helix and coil structures. The confidence scores of its residues ranged between 1 and 9, in which higher scores were more reliable (Fig. 8).

The accuracy of the prediction program is an important criterion for the selection of the best 3-D models. A confidence score (C-score) value in the range of -5 to +2 reflects the confidence of the models, and a C-score>-1.5 is an estimate of the model with a correct fold (Roy et al. 2010; Yang and Zhang 2015). The C-score of the top five generated models of the recombinant SNK-Z by the I-TASSER server ranged between (-4.18) and (-0.20). The first model, with a C-score of -0.20 whom value confirmed the confidence of the model, is shown in Fig. 8. The structural alignment program TM-align from the Protein Data Bank (PDB) library ranked structural analogs based on their template modeling score (Tm-score). This value scales the structural similarity between the predicted model and structures in the PDB. A TM-score > 0.5 reflects that the predicted model and native structure have similar topologies (Roy et al. 2010; Yang and Zhang 2015). The quality of threading alignment

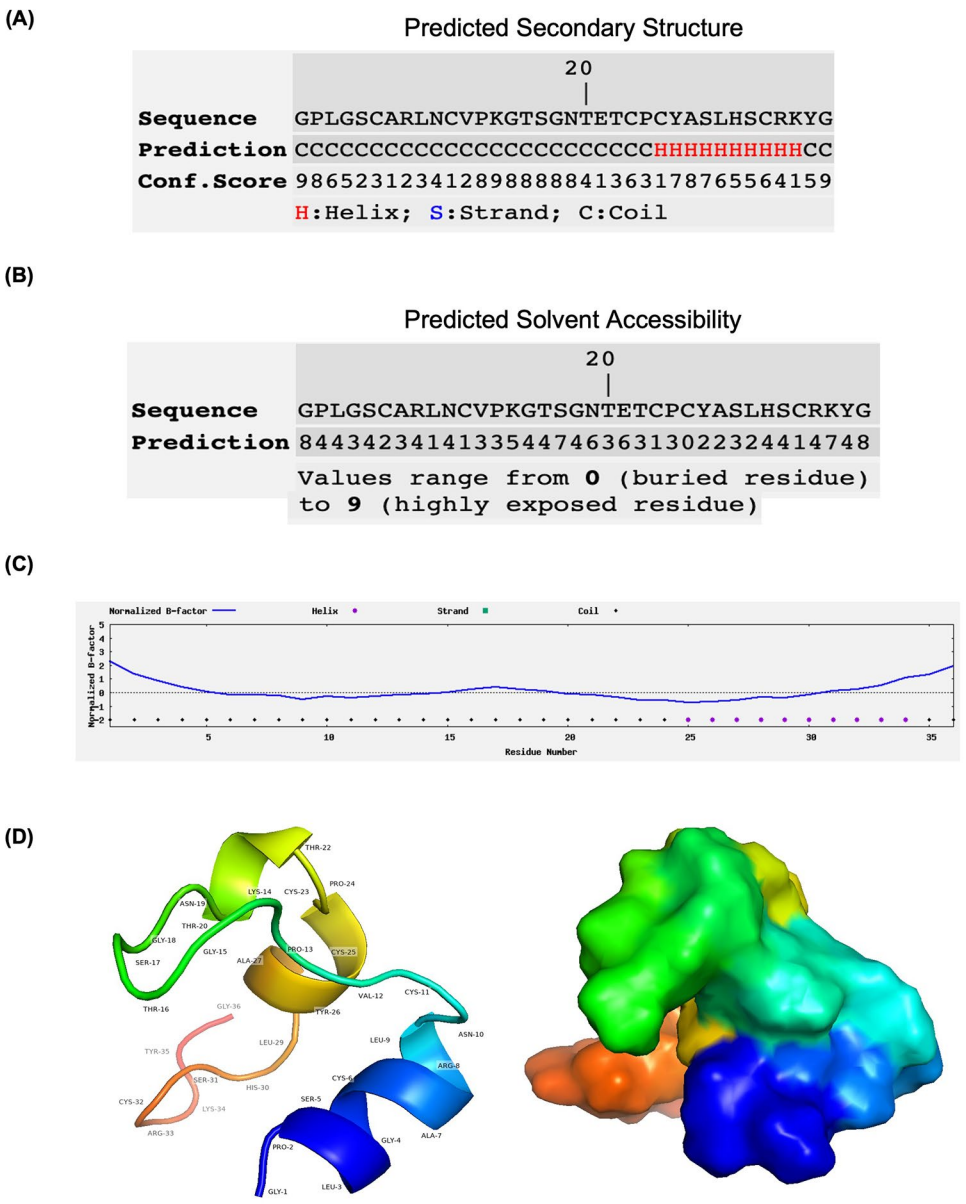

Fig. 8 Prediction of the 3-D structure of SNK-Z with the I-TASSER algorithm. **(A)** Predicted secondary structure of the recombinant SNK-Z peptide, which contains alpha helices (red) and coil structures (black). "H" and "C" indicate helix and coil, respectively. **(B)** The predicted solvent accessibility is presented on 10 levels, from buried (0) to highly exposed (9). **(C)** Prediction of normalized B-factor. Positive normalized B-factors indicate these regions are structurally more flexible whereas negative values and values close to zero suggest these regions are structurally more stable. **(D)** 3-D visualization of the SNK-Z using PyMOL.

was evaluated according to the normalized Z-score. A normalized Z-score > 1 indicates good alignment. Top ten structural analogs in the PDB that were closest to the first I-TASSER model are given in Supplementary Fig. 4 [SI]. The estimated Tm-score of the first model was 0.69 ± 0.12 (Fig. 8). Solvent accessibility is a feature of proteins that determines their folding and stability. This feature is used to predict the normalized B-factor (B-factor profile, BFP). Negative B-factor values indicate that more conserved residues have relatively more stable structures, whereas positive B-factor values indicates less stable structures (Yang and Zhang 2015). The solvent accessibility and normalized B-factor of the recombinant SNK-Z are illustrated in Fig. 8.

Computational modeling is a powerful tool for the prediction of protein structures and functions and the identification of promising candidates with therapeutic potential. Zare-Zardini et al. (2013) reported the potency of SNK-Z to be a putative agent in the treatment of Alzheimer's disease due to its inhibitory activity against acetylcholinesterase and butyrylcholinesterase. The low in vitro hmolytic activity of SNK-Z against human red blood cells shows its potential as a new medical drug, especially as an antimicrobial (Daneshmand et al. 2013). The 3-D structural model predictions of the peptide will support structure-based docking research by providing basic data for wet-lab studies.

Conclusions

Acquired resistance to the traditional antibiotics used in medicine, aquaculture, and the food industry has led to health problems and environmental issues. AMPs have a broad antimicrobial spectrum and show activity with specific mechanisms. Therefore, the acquisition of resistance against peptides in pathogenic microorganisms is lower than that of antibiotics. This is the most important reason why AMPs are preferred rather than the use of traditional antibiotics. To expand the application of AMPs and increase their yield, optimized heterologous systems must be developed. *In silico* analysis can provide valuable insights into the evaluation of molecules that are promising for scientific research and industrial applications. This study is the first to report the production and purification of a recombinant SNK-Z peptide with fusion partners in *E. coli*, as well as the illumination of the structure of the recombinant AMP. Further analysis should be performed to assess the potential of recombinant SNK-Z as a novel antimicrobial agent.

Supplementary Information The online version contains supplementary material available at https://doi.org/10.1007/s10989-023-10556-9.

Acknowledgements The Council of Higher Education (CoHE) is acknowledged for granting of T. Teker's doctoral study in the frame of 100/2000 CoHE Doctoral Scholarship Program. The Scientific and Technological Research Council of Turkey is gratefully acknowledged by T. Teker for granting a fellowship within the scope of the BIDEB 2211-A National PhD Scholarship Program. We extend our thanks to G.B. Albayrak -bilingual-proficient- for grammatically correcting this article.

Author Contributions Conceptualization: [T. Teker, G. Albayrak, K. Turan]; Methodology: [T. Teker, G. Albayrak, K. Turan]; Formal analysis and investigation: [T. Teker, G. Albayrak, K. Turan]; Writing - original draft preparation: [T. Teker]; Writing - review and editing: [G. Albayrak, K. Turan]; Funding acquisition: [G. Albayrak]; Supervision: [G. Albayrak, K. Turan]. All authors read and approved the final manuscript.

Funding This study was funded by Scientific Research Projects Coordination Unit of Istanbul University. Project number:36971.

Declarations

Competing interests The authors declare no competing interests.

Ethical Approval The authors declare that ethical standards have been followed in accordance with the policies of this journal.

References

Berrocal-Lobo M, Segura A, Moreno M, López G, Garcıa-Olmedo F, Molina A (2002) Snakin-2, an antimicrobial peptide from potato whose gene is locally induced by wounding and responds to pathogen infection. Plant Physiol 128:951–961. https://doi.org/10.1104/pp.010685

Bradford MM (1976) A rapid and sensitive method for the quantitation of microgram quantities of protein utilizing the principle of protein-dye binding. Anal Biochem 72:248–254. https://doi.org/10.1016/0003-2697(76)90527-3

Cao W, Liu Q, Wang T, Zhang Q, Cheng F, Tang Y, Mei C, Wen F, Wang W (2021) Recombinant expression of the precursor of rat lung surfactant protein B in *Escherichia coli* and its antibacterial mechanism. Protein Expr Purif 179:105801. https://doi.org/10.1016/j.pep.2020.105801

Chang AY, Chau V, Landas JA, Pang Y (2017) Preparation of calcium competent *Escherichia coli* and heat-shock transformation. JEMI methods 1:22–25

Daneshmand F, Zare-Zardini H, Ebrahimi L (2013) Investigation of the antimicrobial activities of Snakin-Z, a new cationic peptide derived from *Zizyphus jujuba* fruits. Nat Prod Res 27:2292–2296. https://doi.org/10.1080/14786419.2013.827192

Harper S, Speicher DW (2011) Purification of proteins fused to glutathione s-transferase. In: Walls D, Loughran S (eds) Protein chromatography. Methods in molecular biology, vol 681. Humana Press, pp 259–280. https://doi.org/10.1007/978-1-60761-913-0_14

Herbel V, Schäfer H, Wink M (2015) Recombinant production of snakin-2 (an antimicrobial peptide from tomato) in *E. coli* and analysis of its bioactivity. Molecules 20:14889–14901. https://doi.org/10.3390/molecules200814889

Jeyarajan S, Sathyan A, Peter AS, Ranjith S, Duraisamy S, Natarajaseenivasan SM, Chidambaram P, Kumarasamy A (2023) Bioproduction and Characterization of Epinecidin-1 and Its Variants Against Multi Drug Resistant Bacteria Through *In Silico* and *In Vitro* Studies. Int J Pept Res Ther 29:66. https://doi.org/10.1007/s10989-023-10537-y

Li J, Hu S, Jian W, Xie C, Yang X (2021) Plant antimicrobial peptides: structures, functions, and applications. Bot Stud 62:5. https://doi.org/10.1186/s40529-021-00312-x

Liu S, Bao J, Lao X, Zheng H (2018) Novel 3D structure based model for activity prediction and design of antimicrobial peptides. Sci Rep 8:11189. https://doi.org/10.1038/s41598-018-29566-5

Merril CR, Dunau ML, Goldman D (1981) A rapid sensitive silver stain for polypeptides in polyacrylamide gels. Anal Biochem 110:201–207. https://doi.org/10.1016/0003-2697(81)90136-6

Roy A, Kucukural A, Zhang Y (2010) I-TASSER: a unified platform for automated protein structure and function prediction. Nat Protoc 5:725–738. https://doi.org/10.1038/nprot.2010.5

Segura A, Moreno M, Madueño F, Molina A, García-Olmedo F (1999) Snakin-1, a peptide from potato that is active against plant pathogens. Mol Plant Microbe Interact 12:16–23. https://doi.org/10.1094/MPMI.1999.12.1.16

Su T, Han M, Cao D, Xu M (2020) Molecular and biological properties of snakins: the foremost cysteine-rich plant host defense peptides. J Fungi 6:220. https://doi.org/10.3390/jof6040220

Taghizadeh S, Savardashtaki A, Irajie C, Rahbar MR, Ghasemi Y (2022) Recombinant expression and antibacterial properties of BmTXKS2 venom peptide in fusion with GST. Int J Pept Res Ther 28:66. https://doi.org/10.1007/s10989-022-10374-5

Wang G (2020) The antimicrobial peptide database provides a platform for decoding the design principles of naturally occurring antimicrobial peptides. Protein Sci 29:8–18. https://doi.org/10.1002/pro.3702

Wheeler JI, Irving HR (2012) Plant peptide signaling: an evolutionary adaptation. In: Irving H, Gehring C (eds) Plant signaling peptides. Signaling and communication in plants, vol 16. Springer, Berlin, Heidelberg, pp 1–23. https://doi.org/10.1007/978-3-642-27603-3_1

Wirjanata G, Handayuni I, Zaloumis SG, Chalfein F, Prayoga P, Kenangalem E, Poespoprodjo JR, Noviyanti R, Simpson JA, Price RN, Marfurt J (2016) Analysis of *ex vivo* drug response data of *Plasmodium* clinical isolates: the pros and cons of different computer programs and online platforms. Malar J 15:1–10. https://doi.org/10.1186/s12936-016-1173-1

Yang J, Zhang Y (2015) I-TASSER server: new development for protein structure and function predictions. Nucleic Acids Res 43:W174–W181. https://doi.org/10.1093/nar/gkv342

Yeung H, Squire CJ, Yosaatmadja Y, Panjikar S, López G, Molina A, Baker EN, Harris PWR, Brimble MA (2016) Radiation damage and racemic protein crystallography reveal the unique structure of the GASA/snakin protein superfamily. Angew Chem 128:8062–8065. https://doi.org/10.1002/ange.201602719

Yu W, Gao XJ, Liu Y, Wang Q (2016) Fusion expression of cecropin B-like antibacterial peptide in *Pichia* GS115 and its antibacterial mechanism. Biotechnol Lett 38:305–312. https://doi.org/10.1007/s10529-015-1978-y

Zare-Zardini H, Tolueinia B, Hashemi A, Ebrahimi L, Fesahat F (2013) Antioxidant and cholinesterase inhibitory activity of a new peptide from *Ziziphus jujuba* fruits. Am J Alzheimer's Dis Other Demen 28:702–709. https://doi.org/10.1177/1533317513500839

Zhang QY, Yan ZB, Meng YM, Hong XY, Shao G, Ma JJ, Cheng XR, Liu J, Kang J, Fu CY (2021) Antimicrobial peptides: mechanism of action, activity and clinical potential. Military Med Res 8:48. https://doi.org/10.1186/s40779-021-00343-2